Journal of Physics and Chemistry of Solids 136 (2020) 109127

Contents lists available at ScienceDirect

Journal of Physics and Chemistry of Solids

journal homepage: www.elsevier.com/locate/jpcs

Effect of confined longitudinal optical-phonons on cyclotron resonance absorption full width at half maximum in quantum wells

Le Thi Thu Phuong[a], Le Dinh[a], Nguyen Dinh Hien[b,c,*]

[a] Center for Theoretical and Computational Physics, University of Education, Hue University, Hue City, Viet Nam
[b] Laboratory of Magnetism and Magnetic Materials, Advanced Institute of Materials Science, Ton Duc Thang University, Ho Chi Minh City, Viet Nam
[c] Faculty of Applied Sciences, Ton Duc Thang University, Ho Chi Minh City, Viet Nam

ARTICLE INFO

Keywords:
Cyclotron resonance
Full width at half maximum
Longitudinal optical-confined phonon
Quantum well

ABSTRACT

In this study, using the projection operator method, we investigated the influence of longitudinal optical (LO)-phonon confinement on the cyclotron resonance (CR) effect in quantum wells by calculating the expression for the absorption power. The full width at half maximum (FWHM) was obtained for the CR peaks using a computational method. The numerical results were determined for GaAs quantum wells based on three models of confined phonons delineated by Ridley, Fuchs–Kliewer, and Huang–Zhu, and for the bulk phonons. The CR absorption FWHM increased as the magnetic field and temperature increased, but decreased as the well width increased. These results are in good agreement with those obtained theoretically by Singh and Kobori et al. In addition, the CR absorption FWHM had a smaller value for the bulk phonons and it changed more slowly than that for the confined phonons. Furthermore, the CR absorption FWHM was largest for the Huang-Zhu model among the three models of confined phonons, and smallest for the Ridley model. These results are also in agreement with those obtained theoretically by Rudin et al. Weber et al., and Bhat et al. In addition, phonon confinement was determined as very important over the small range of the well width and it should be considered when investigating the CR absorption FWHM.

1. Introduction

Cyclotron resonance (CR) occurs in semiconductors in the presence of both electric and magnetic fields, and the electric field frequency (photon frequency) is equal to the cyclotron frequency, i.e., the photon energy is equal to the cyclotron energy. The conditions and characteristics of this phenomenon depend on the temperature, magnetic field strength, and nature of the carrier scattering mechanism. Thus, this effect allows us to obtain much direct information about the effective mass, scattering processes, and non-parabolicity of the valence and conduction bands [1]. The CR effect has been studied both theoretically [2] and experimentally [3] in bulk semiconductors, and experimentally in quantum wells [4–6] under the bulk phonon assumption. CR effects in quasi-two-dimensional electron systems have been studied widely because electron–phonon interactions are the main type of interaction in high-purity semiconductors. It is useful to clarify the new properties of two-dimensional electron gases due to their application in an external field, thereby providing information about the crystals and optical properties of quasi-two-dimensional electron systems for manufacturing optoelectronics and electronics devices. At present, physicists are particularly interested in studying low-dimensional semiconductors in general and quantum wells, and detecting new effects that have not been thoroughly investigated to find more features in familiar effect due to electron-phonon interaction identify more features due to electron–phonon interactions caused by high frequency fields such as CR effects when considering confined phonons. Phonon confinement is necessary whenever the phonon coherence length is larger than the width of a quantum well [7] and it should be considered to obtain realistic estimates of confined electron–phonon scattering [8]. The confined phonon effect is a necessary component of electron-phonon interactions and it causes an increase in electron–phonon scattering rates as well as modifying the density of states for phonons in low-dimensional semiconductor structures [7,9,10]. Several models have been proposed of phonon confinement due to different lattice dynamic boundary conditions in quantum wells, such as those developed by Ridley (R) [11], Fuchs and Kliewer (FK) [12,13], and Huang and Zhu (HZ) [14,15]. The CR absorption full width at half maximum (FWHM) is useful for studying the transport behavior and scattering

* Corresponding author. Laboratory of Magnetism and Magnetic Materials, Advanced Institute of Materials Science, Ton Duc Thang University, Ho Chi Minh City, Viet Nam.
E-mail address: nguyendinhhien@tdtu.edu.vn (N.D. Hien).

https://doi.org/10.1016/j.jpcs.2019.109127
Received 30 January 2019; Received in revised form 31 July 2019; Accepted 1 August 2019
Available online 04 August 2019

mechanisms of carriers in materials [3,16,17]. Hence, it may be used to probe the confined electron-confined longitudinal optical (LO)-phonon scattering process. The FWHM of the CR peak due to electron–bulk LO-phonon interactions has been studied, but further research is required to understand the situation when confined LO-phonons are considered. The FWHM is defined as the profile of the curves describing the dependence of the absorption power on the photon energy [16,18,19]. The FWHM has been measured in quantum wells [20–24], quantum wires [25–27], quantum dots [28–30], monolayer molybdenum disulfide [31], and a MoS_2 monolayer on polar substrates [19]. However, the FWHM was determined for bulk phonons in these previous studies. Only a few studies have investigated the confined phonon effect [8,32–34]. Thus, it is necessary to study the LO-phonon confinement effects on the CR absorption FWHM. In the present study, we investigated the FWHM of the CR peak for the three previously mentioned models of phonons in quantum wells. We determined the dependence of the CR absorption FWHM on the width of the well, temperature of the system, and magnetic field by using the projection operator method is presented to compare. This work. The remainder of this study is organized as follows. In Section 2, we introduce the different models of confined phonons in quantum wells and their basic formulations. In Section 3, we calculate the absorption power in quantum wells due to confined LO-phonons. In Section 4, we present and discuss the numerical results obtained for GaAs quantum wells. Finally, we give our conclusions in Section 5.

2. Analytic results for matrix element electron–confined phonon interactions in quantum wells

In this study, we consider a quantum well where an electron is free in the $x-y$ plane and confined in the potential barrier $V(z)$, $V(z)=0$ for $|z|<L_z/2$ and $V(z)=\infty$ for $|z|>L_z/2$. Assuming that a magnetic field, $\mathbf{B}=(0,0,B)$, is applied in the z direction and the Landau gauge of vector potential is $\mathbf{A}=(0,xB,0)$, then one electron eigenfunction $\Psi(Nnk_y)$ and the energy eigenvalues $E(Nn)$ are given by Ref. [33]:

$$\Psi(Nnk_y)=\frac{1}{\sqrt{L_y}}\psi_N(x-x_0)\exp(ik_y y)\phi_n(z), \tag{1}$$

$$E(Nn)=(N+1/2)\hbar\omega_{cy}+n^2\varepsilon_0, \tag{2}$$

where $N=0,1,2,\cdots$ is the Landau level index, $n=1,2,3,\cdots$ is the electric subband index, $\psi_N(x-x_0)$ is the harmonic oscillator wave function centered at $x_0=-b_c^2k_y$ with $b_c=(\hbar c/eB)^{1/2}$, k_y is the cyclotron radius and the wave vector of the electron is in y-direction; L_y, and $\phi_n(z)$ are the normalization length and electron wave function, respectively; $\omega_c=eB/m^*$ and $\varepsilon_0=\hbar^2\pi^2/(2m^*L_z^2)$ are the cyclotron frequency and energy of the lowest electric subband with L_z; m^* is the width of the well, and the effective mass of an electron $\phi_n(z)$ is given by Ref. [33]:

$$\phi_n(z)=\sqrt{\frac{2}{L_z}}\sin\left(\frac{n\pi z}{L_z}+\frac{n\pi}{2}\right). \tag{3}$$

The matrix element for the confined electron–confined LO-phonon interaction can be written as [8,15,33]:

$$|\langle i|H_{el-ph}|f\rangle|^2=\frac{e^2\hbar\omega_{LO}\chi^*}{2\varepsilon_0V_0}|V_{\ell\theta}^{\zeta}(q_\perp)|^2|J_{NN'}(u)|^2|G_{n_i,n_f}^{\zeta,\ell\theta}|^2\delta_{k_\perp^f,k_\perp^i\pm q_\perp}, \tag{4}$$

where ζ (= R, FK, HZ) are the models of confined phonons in quantum wells:

$$|J_{NN'}(u)|^2=\frac{n_2!}{n_1!}e^{-u}u^{n1-n2}\left[L_{n2}^{n1-n2}(u)\right]^2, \tag{5}$$

$u=b_c^2q_\perp^2/2$; L_{n2}^{n1-n2} is the Laguerre polynomial, $n1=max\{N,N'\}$, and $n2=min\{N,N'\}$.

$$G_{n_i,n_f}^{\zeta,\ell\theta}=\int_{-L_z/2}^{L_z/2}\phi_{n_f}^*(z)u_{\ell\theta}^{\zeta}(z)\phi_{n_i}(z)dz \tag{6}$$

is the overlap integral [8] with the inter-subband and intra-subband; $\chi^*=(1/\chi_\infty-1/\chi_0)$, where χ_0 and χ_∞ are the static and high-frequency dielectric constants, respectively; ε_0 is the vacuum dielectric constant, $\mathbf{q}_\perp=(q_x,q_y)$ is the two-dimensional LO-phonon wave vector, $V_0=SL_z$, and $\hbar\omega_{LO}=36.25$ meV is the energy of the LO-phonon in the GaAs quantum well. In the confined space, $u_{\ell\theta}^{\zeta}(z)$ is the parallel composition of the displacement vector for the $\ell-$th phonon mode, and it is different for the R [11], FK [13], and HZ [15] models, where θ denotes the (+) odd and (−) even phonon confinement modes. For the R model, $u_{\ell\theta}^{\zeta}(z)$ is written as follows:

$$u_{\ell+}^{R}(z)=\sin\left(\frac{\ell\pi z}{L_z}\right),\ \ell=1,3,5,\ \cdots, \tag{7}$$

$$u_{\ell-}^{R}(z)=\cos\left(\frac{\ell\pi z}{L_z}\right),\ \ell=2,4,6,\ \cdots. \tag{8}$$

For the FK model:

$$u_{\ell+}^{FK}(z)=\cos\left(\frac{\ell\pi z}{L_z}\right),\ \ell=1,3,5,\ \cdots, \tag{9}$$

$$u_{\ell-}^{FK}(z)=\sin\left(\frac{\ell\pi z}{L_z}\right),\ \ell=2,4,6,\ \cdots. \tag{10}$$

For the HZ model:

$$u_{\ell+}^{HZ}(z)=\sin\left(\frac{\mu_\ell\pi z}{L_z}\right)+\frac{c_\ell z}{L_z},\ \ell=3,5,7,\ \cdots, \tag{11}$$

$$u_{\ell-}^{HZ}(z)=\cos\left(\frac{\mu_\ell\pi z}{L_z}\right)-(-1)^{\ell/2},\ \ell=2,4,6,\ \cdots, \tag{12}$$

where μ_ℓ and c_ℓ are given by:

$$\tan\left(\frac{\mu_\ell\pi}{2}\right)=\frac{\mu_\ell\pi}{2},\ \ell-1<\mu_\ell<\ell, \tag{13}$$

$$c_\ell=-2\sin\left(\frac{\mu_\ell\pi}{2}\right). \tag{14}$$

The term $V_{\ell\theta}^{\zeta}(q_\perp)$ in Eq. (4) is given by Ref. [33]:

$$V_{\ell\theta}^{\zeta}(q_\perp)=(a_{\ell\theta}^{\zeta}q_\perp^2+b_{\ell\theta}^{\zeta}/L_z^2)^{-1/2}, \tag{15}$$

with $a_{\ell\theta}^{HZ}$ and $b_{\ell\theta}^{HZ}$ for the HZ model is:

$$a_{\ell+}^{HZ}=1+c_\ell^2\left(\frac{1}{6}-\frac{1}{\mu_\ell^2\pi^2}\right),\ b_{\ell+}^{HZ}=\mu_\ell^2\pi^2-c_\ell^2,\ \ell=3,5,7,\ \cdots, \tag{16}$$

$$a_{\ell-}^{HZ}=3,\ b_{\ell-}^{HZ}=\ell^2\pi^2,\ \ell=2,4,6,\ \cdots, \tag{17}$$

and these factors are

$$a_{\ell\pm}^{FK,R}=1,\ b_{\ell\pm}^{FK,R}=\ell^2\pi^2,\ \ell=1,2,3,\ \cdots, \tag{18}$$

for the FK and R models.

Eq. (6) can be evaluated for the inter-subband transition ($1\rightarrow 2$) and intra-subband transition ($1\rightarrow 1$) using all three models of phonon confinement. For the R model, we can obtain:

$$\begin{aligned}
&G_{12}^{R,\ell+}=-\tfrac{1}{2}(\delta_{m,1}+\delta_{\ell,3}),\ \ell=1,3,5,\cdots,\\
&G_{12}^{R,\ell-}=0,\ \ell=2,4,6,\cdots,\\
&G_{11}^{R,\ell+}=0,\ \ell=1,3,5,\cdots,\\
&G_{11}^{R,\ell-}=\tfrac{1}{2}\delta_{\ell,2},\ \ell=2,4,6,\ \cdots.
\end{aligned} \tag{19}$$

For the FK model, we have:

$$G_{12}^{FK,\ell+} = 0,\ \ell = 1,3,5,\cdots,$$
$$G_{12}^{FK,\ell-} = -\frac{2}{\pi}\ell(-1)^{\ell/2}\left[\frac{1}{\ell^2-9} - \frac{1}{\ell^2-1}\right],\ \ell = 2,4,6,\cdots,$$
$$G_{11}^{FK,\ell+} = -2(-1)^{(\ell+1)/2}\left[\frac{1}{\ell\pi} + \frac{\ell\pi}{4\pi^2-\pi^2\ell^2}\right],\ \ell = 1,3,5,\cdots,$$
$$G_{11}^{FK,\ell-} = 0,\ \ell = 2,4,6,\ \cdots. \tag{20}$$

For the HZ model, we have:

$$G_{12}^{HZ,\ell+} = -\frac{2c_\ell}{\pi^2}\left\{\frac{8}{9} + \left[\frac{1}{\mu_\ell^2-1} - \frac{1}{\mu_\ell^2-9}\right]\right\},\ \ell = 3,5,7,\cdots,$$
$$G_{12}^{HZ,\ell-} = 0,\ \ell = 2,4,6,\cdots,$$
$$G_{11}^{HZ,\ell+} = 0,\ \ell = 3,5,7,\cdots,$$
$$G_{11}^{HZ,\ell-} = \frac{3}{2}\delta_{\ell,2} - (-1)^{\ell/2}(1-\delta_{\ell,2}),\ \ell = 2,4,6,\ \cdots. \tag{21}$$

The analytic results show that only even modes in the HZ model, odd modes in the FK model, and the $\ell = 2$ mode in the R model contribute to the intra-subband transition. However, only odd modes in the HZ model, even modes in the FK model, and the $\ell = 1,3$ modes in the R model contribute to the inter-subband transition.

3. Effect of confined phonons on the magneto-optical absorption power in quantum wells

The average magneto-optical absorption power, P, per unit volume of a quantum well delivered by an electromagnetic wave with amplitude, E_0, and a circularly polarized microwave with a frequency, ω, is given by Ref. [35]:

$$P(\omega) = \frac{E_0^2}{2\hbar\omega}\sum_\alpha \frac{|j_\alpha^+|^2(f_\alpha - f_{\alpha+1})\gamma(\omega)}{(\omega-\omega_c)^2 + [\gamma(\omega)]^2}, \tag{22}$$

where f_α and $f_{\alpha+1}$ are the Fermi–Dirac distribution functions for an electron in state $|\alpha\rangle = |N, n, k_y\rangle$ and $|\alpha+1\rangle = |N+1, n, k_y\rangle$; and E_0 and ω are the amplitude and frequency of the electromagnetic field, respectively:

$$|j_\alpha^+|^2 = |\langle\alpha+1|j^+|\alpha\rangle|^2 = 2e^2\hbar\omega_c(N+1)/m^*. \tag{23}$$

The term $\gamma(\omega)$ in Eq. (22) for bulk LO-phonons is obtained by Ref. [36]:

$$\begin{aligned}\gamma(\omega) &\equiv \gamma^{bp}(\omega)\\ &= \sum_{N'}\sum_{n'}\frac{C^b I_{nn'}}{(f_{N+1,n}-f_{N,n})}\int_0^\infty dq_\perp \frac{|J_{N,N'}(u)|^2}{q_\perp}\\ &\times\{[(1+N_{\mathbf{q}})f_{N+1,n}(1-f_{N',n'}) - N_{\mathbf{q}}f_{N',n'}(1-f_{N+1,n})]\delta(E_1^-)\\ &+ [N_{\mathbf{q}}f_{N+1,n}(1-f_{N',n'}) - (1+N_{\mathbf{q}})f_{N',n'}(1-f_{N+1,n})]\delta(E_1^+)\}\\ &+ \sum_{N'}\sum_{n'}\frac{C^b I_{nn'}}{(f_{N+1,n}-f_{N,n})}\int_0^\infty dq_\perp \frac{|J_{N+1,N'}(u)|^2}{q_\perp}\\ &\times\{[(1+N_{\mathbf{q}})f_{N',n'}(1-f_{N,n}) - N_{\mathbf{q}}f_{N,n}(1-f_{N',n'})]\delta(E_2^-)\\ &+ [N_{\mathbf{q}}f_{N',n'}(1-f_{N,n}) - (1+N_{\mathbf{q}})f_{N,n}(1-f_{N',n'})]\delta(E_2^+)\}\end{aligned} \tag{24}$$

where

$$C^b = \frac{e^2\hbar\omega_{LO}\chi^*}{8\pi\hbar\varepsilon_0}, \tag{25}$$

$$I_{nn'} = \frac{\pi}{L_z}(2+\delta_{n,n'}), \tag{26}$$

$$E_1^\pm = \hbar\omega + (N'-N-1)\hbar\omega_c + (n'^2-n^2)\varepsilon_0 \pm \hbar\omega_{LO}, \tag{27}$$

$$E_2^\pm = \hbar\omega + (N-N')\hbar\omega_c + (n^2-n'^2)\varepsilon_0 \pm \hbar\omega_{LO}, \tag{28}$$

($\delta(E_m^\pm)$, $m = 1,2$) in Eq. (24) are the Dirac's delta functions, which are replaced by Lorentzians of width $\gamma_{N,N'}^\pm$, $\gamma_{N+1,N'}^\pm$, i.e. [37]:

$$\delta(E_1^\pm) = \frac{1}{\pi}\frac{\gamma_{N,N'}^\pm}{(E_1^\pm)^2 + (\gamma_{N,N'}^\pm)^2},\ \delta(E_2^\pm) = \frac{1}{\pi}\frac{\gamma_{N+1,N'}^\pm}{(E_2^\pm)^2 + (\gamma_{N+1,N'}^\pm)^2}, \tag{29}$$

with

$$(\gamma_{N',N}^\pm)^2 = \frac{C^b\hbar}{\pi}\left(N_{\mathbf{q}} + \frac{1}{2} \pm \frac{1}{2}\right)I_{nn'}\int_0^\infty dq_\perp \frac{|J_{N,N'}(u)|^2}{q_\perp}, \tag{30}$$

$$(\gamma_{N+1,N'}^\pm)^2 = \frac{C^b\hbar}{\pi}\left(N_{\mathbf{q}} + \frac{1}{2} \pm \frac{1}{2}\right)I_{nn'}\int_0^\infty dq_\perp \frac{|J_{N+1,N'}(u)|^2}{q_\perp}. \tag{31}$$

The term $\gamma(\omega)$ in Eq. (22) for confined LO-phonons is obtained by Ref. [36]:

$$\begin{aligned}\gamma(\omega) &\equiv \gamma^{cp}(\omega)\\ &= \sum_{N',n'}\sum_\ell\sum_{\theta=\pm}\frac{C^c G_{n',n}^{\zeta,\ell\theta}}{(f_{N+1,n}-f_{N,n})}\int_0^\infty q_\perp dq_\perp \frac{J_{N,N'}}{a_{\ell\theta}^\zeta q_\perp^2 + \frac{b_{\ell\theta}^\zeta}{L_z^2}}\\ &\times\{[(1+N_{\mathbf{q}})f_{N+1,n}(1-f_{N',n'}) - N_{\mathbf{q}}f_{N',n'}(1-f_{N+1,n})]\delta(E_1^-)^{cf}\\ &+ [(1+N_{\mathbf{q}})f_{N',n'}(1-f_{N+1,n}) - N_{\mathbf{q}}f_{N+1,n}(1-f_{N',n'})]\delta(E_1^+)^{cf}\}\\ &+ \sum_{N',n'}\sum_\ell\sum_{\theta=\pm}\frac{C^c G_{n,n'}^{\zeta,\ell\theta}}{(f_{N+1,n}-f_{N,n})}\int_0^\infty q_\perp dq_\perp \frac{J_{N+1,N'}}{a_{\ell\theta}^\zeta q_\perp^2 + \frac{b_{\ell\theta}^\zeta}{L_z^2}}\\ &\times\{[(1+N_{\mathbf{q}})f_{N',n'}(1-f_{N,n}) - N_{\mathbf{q}}f_{N,n}(1-f_{N',n'})]\delta(E_2^-)^{cf}\\ &+ [(1+N_{\mathbf{q}})f_{N,n}(1-f_{N',n'}) - N_{\mathbf{q}}f_{N',n'}(1-f_{N,n})]\delta(E_2^+)^{cf}\}\end{aligned} \tag{32}$$

where $N_{\mathbf{q}}$ is the Planck distribution function in the state $|q\rangle = |\ell, q_\perp\rangle$ for confined LO-phonon,

$$C^c = \frac{e^2\hbar\omega_{LO}^{\ell,q_\perp}\chi^*}{8\pi\hbar\varepsilon_0 L_z}, \tag{33}$$

$$E_1^\pm = \hbar\omega + (N'-N-1)\hbar\omega_c + (n'^2-n^2)\varepsilon_0 \pm \hbar\omega_{LO}^{\ell,q_\perp}, \tag{34}$$

$$E_2^\pm = \hbar\omega + (N-N')\hbar\omega_c + (n^2-n'^2)\varepsilon_0 \pm \hbar\omega_{LO}^{\ell,q_\perp}, \tag{35}$$

$$\delta(E_1^\pm)^{cf} = \frac{1}{\pi}\frac{\gamma_{N,N'}^{\zeta\pm}}{(E_1^\pm)^2 + (\gamma_{N,N'}^{\zeta\pm})^2},\ \delta(E_2^\pm)^{cf} = \frac{1}{\pi}\frac{\gamma_{N+1,N'}^{\zeta\pm}}{(E_2^\pm)^2 + (\gamma_{N+1,N'}^{\zeta\pm})^2}, \tag{36}$$

where:

$$\begin{aligned}&(\gamma_{N',N}^{\zeta\pm})^2\\ &= \frac{C^c}{\pi\hbar S}\left(N_q + \frac{1}{2} \pm \frac{1}{2}\right)\sum_\ell\sum_{\theta=\pm}|G_{n',n}^{\zeta,\ell\theta}|^2\int_0^\infty q_\perp dq_\perp \frac{J_{N,N'}}{a_{\ell\theta}^\zeta q_\perp^2 + \frac{b_{\ell\theta}^\zeta}{L_z^2}},\end{aligned} \tag{37}$$

$$\begin{aligned}&(\gamma_{N+1,N'}^{\zeta\pm})^2\\ &= \frac{C^c}{\pi\hbar S}\left(N_q + \frac{1}{2} \pm \frac{1}{2}\right)\sum_\ell\sum_{\theta=\pm}|G_{n,n'}^{\zeta,\ell\theta}|^2\int_0^\infty q_\perp dq_\perp \frac{J_{N+1,N'}}{a_{\ell\theta}^\zeta q_\perp^2 + \frac{b_{\ell\theta}^\zeta}{L_z^2}}.\end{aligned} \tag{38}$$

4. Numerical results and discussion

We obtained the absorption power in a square GaAs quantum well as a function of the photon energy. The material parameters used are [38]: $\varepsilon_0 = 8.85\times10^{-12}\ C^2/Nm^2$, $\chi_0 = 13.18$, $\chi_\infty = 10.89$, $\hbar\omega_{LO} = 36.25$ meV, $E_0 = 5.0\times10^6$ V/m, and $m^* = 0.067\times m_0$ (m_0 is the mass of a free electron). We assumed that $N = 0$, $N' = 1$ only for the Landau levels and that $n = 1$, $n' = 1,2$ for electron confinement were occupied by electrons, and the result was considered in the quantum limit.

Fig. 1(a) shows the dependence of the magneto-optical absorption power in a square GaAs quantum well on the photon energy at $T = 300$ K, $B = 10$ T, and $L_z = 12$ nm for bulk phonons (solid curve) and phonon confinement described by the R (dashed-dotted curve), FK (dotted curve), and HZ (dashed curve) models. Each curve contained five peaks corresponding to the ODMPR for intra-subband transitions (1-1) and inter-subband transitions (1–2). The CR peak satisfies the condition $\hbar\omega = (N'-N)\hbar\omega_c$.

The first peak at $\hbar\omega = 17.28$ meV corresponds to the condition where $\hbar\omega = (N'-N)\hbar\omega_c$, i.e., 17.28 meV= $(1-0)\times17.28$ meV. This peak indicates that an electron at level $N = 0$ moving to level $N' = 1$

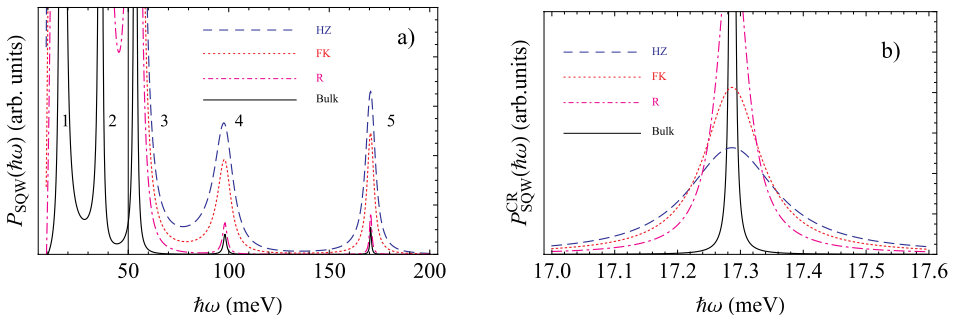

Fig. 1. (a) Effect of photon energy on the magneto-optical absorption power in a square GaAs quantum well at $T = 300$ K, $B = 10$ T, and $L_z = 12$ nm for the different phonon models. Figure (b) is at the 1 peak (CR peak) in the Fig. (a).

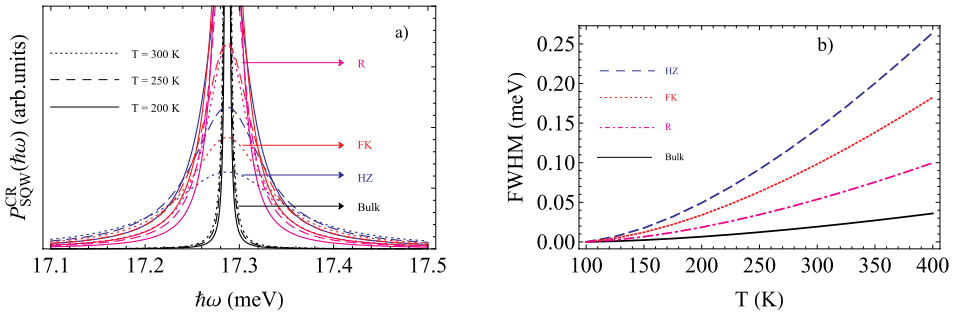

Fig. 2. (a) Magneto-optical absorption power at the CR peak according to four different phonon models at various temperatures. (b) Effect of temperature on the CR absorption FWHM of the CR peak at $B = 10$ T and $L_z = 12$ nm according to the four phonon models.

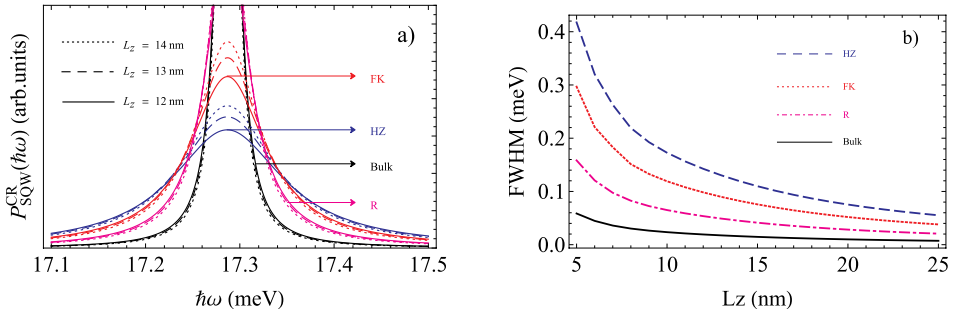

Fig. 3. (a) Magneto-optical absorption power at the CR peak according to the four phonon models for different widths of the well(b) Effects of the well width on the absorption FWHM of the CR peak at $B = 10$ T and $T = 300$ K according to the four phonon models.

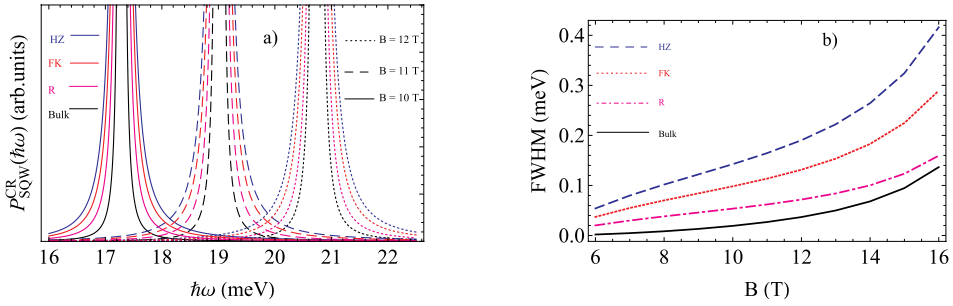

Fig. 4. (a) Magneto-optical absorption power at the CR peak according to the four phonon models at different values of the magnetic field. (b) Effect of the magnetic field on the absorption FWHM of the CR peak at $L_z = 12$ nm and $T = 300$ K according to the four phonon models.

due to the absorption of a photon with energy $\hbar\omega$ and it is called the CR peak.

The second peak at $\hbar\omega = 36.25$ meV corresponds to the condition where $\hbar\omega = \hbar\omega_{LO}$ and it describes the transition of an electron between intra-electric subbands.

The third peak at $\hbar\omega = 53.53$ meV corresponds to the condition where $\hbar\omega = (N' - N)\hbar\omega_c + \hbar\omega_{LO}$, i.e., 53.53 meV= $(1 - 0) \times 17.28$ meV $+ 36.25$ meV, and it describes an electron at level $N = 0$ moving to level $N' = 1$ due to the absorption of a photon with energy $\hbar\omega$ together with the emission of an LO-phonon with energy $\hbar\omega_{LO}$. This is referred to as the optically detected magneto-phonon resonance (ODMPR)peak for the transition between Landau levels.

The fourth peak at $\hbar\omega = 98.12$ meV corresponds to the condition where $\hbar\omega = (N' - N)\hbar\omega_c + (n'^2 - n^2)\varepsilon_0 - \hbar\omega_{LO}$, i.e., 98.12 meV =

$(1-0)\times 17.28 + (2^2-1^2)\times 39.03$ meV $-$ 36.25 meV, and it describes an electron at level $N=0$ moving to level $N'=1$ and from that at level $n=1$ moving to level $n'=2$ due to the absorption of a photon with energy $\hbar\omega$ together with the absorption of an LO-phonon with energy $\hbar\omega_{LO}$. This is referred to as the ODMPR peak for both the transition between Landau levels and the transition between inter-electric subbands.

The fifth peak at $\hbar\omega = 170.62$ meV corresponds to the condition where $\hbar\omega = (N'-N)\hbar\omega_c + (n'^2-n^2)\varepsilon_0 + \hbar\omega_{LO}$, i.e., $170.62\,\text{meV} = (1-0)\times 17.28 + (2^2-1^2)\times 39.03$ meV + 36.25 meV, and it describes an electron at level $N=0$ moving to level $N'=1$ and that at level $n=1$ moving to level $n'=2$ due to the absorption of a photon with energy $\hbar\omega$ together with the emission of an LO-phonon with energy $\hbar\omega_{LO}$. This is referred to as the ODMPR peak for both the transition between Landau levels and the transition between inter-electric subbands.

Fig. 1(b) shows the first peak in Fig. 1(a)) called the CR peak. We used this peak to measure the CR absorption FWHM in a square GaAs quantum well under the effects of the phonon delineated by four models.

Fig. 2(a) shows that the temperature of system does not affect the position of the CR peak but the value of the CR peak is affected by the phonon distribution functions, $N_{\mathbf{q}}$, and electron, $f_{N+1,n}$, $f_{N,n}$. The temperature increases as the value of the CR peak increases while its position is constant because the temperature of system increases with the possibility of electron–phonon scattering, as also shown in a previous theoretical study [39].

Fig. 2(b) shows that the absorption FWHM for the CR peak increases with the system's temperature under all of the phonon models because the temperature of the system increases with the possibility of electron–phonon scattering. Furthermore, the absorption FWHM of the CR peak is smaller for the bulk phonon and it changes more slowly compared with the three confined phonon models because the possibility of electron–phonon scattering increases when a phonon is confined. The CR absorption FWHM is largest with the HZ model among the three confined phonon models (R, FK, and HZ models), but smallest with the R model, as also found in previous theoretical studies [8,40].

Fig. 3(b) shows that the CR absorption FWHM of the CR peak decreases with the rise of the width of well as the well width increases for both the bulk and confined phonons because as the well width increases, the possibility of electron–phonon scattering decreases. Furthermore, the absorption FWHM of the CR peak is smaller for the bulk phonon and it changes more slowly than that with all three confined phonon models because the possibility of electron–phonon scattering increases when a phonon is confined. The CR absorption FWHM is largest for the HZ model among the three confined phonon models (R, FK, and HZ models), but smallest for the R model, as also shown in previous theoretical studies [8,40]. In addition, the absorption FWHM of the CR peak decreases rapidly as the well width increases from $L_z = 5$ nm to $L_z = 25$ nm with all the phonon models. Therefore, when the well width is narrow, phonon confinement becomes more necessary and it should be considered when investigating the CR absorption FWHM. The effect of a confined phonon is negligible on the absorption FWHM of the CR peak in square GaAs quantum wells and it can be ignored when $L_z > 25$ nm.

Fig. 4(b) shows that the absorption FWHM of the CR peak increases as the magnetic field increases for both the bulk and confined phonons because the magnetic field increases with the possibility of electron–phonon scattering. Furthermore, the absorption FWHM of the CR peak is smaller for the bulk phonon and it changes more slowly than that with all three confined phonon models because the possibility of electron–phonon scattering increases when a phonon is confined. The CR absorption FWHM is largest for the HZ model among the three confined phonon models but smallest for the R model, as also shown in previous theoretical investigations [8,40]. In addition, the absorption FWHM of the CR peak increases rapidly when the value of the magnetic field $B \geq 6$ T with all of the phonon models. Therefore, phonon confinement becomes more necessary when the value of the magnetic field $B \geq 6$ T and it should be considered when investigating the CR absorption FWHM, as also found in previous studies of semiconductor quantum wells [4,5,41].

5. Conclusion

In this study, we investigated CR absorption and the effect of phonon confinement on the CR by using the projection operator method. The absorption power was calculated for the R, FK, and HZ confined phonon models. The numerical results indicate that the CR absorption FWHM increases as the magnetic field and temperature increases, whereas it decreases as the well width increases with all of the phonon models, and these results are in good agreement with previous theoretical and experimental results [3,4,42]. In addition, the CR absorption FWHM is smaller for the bulk phonons and it changes more slowly than that for the confined phonons. Furthermore, the CR absorption FWHM is largest for the HZ model among the three confined phonon models (R, FK, and HZ models) and smallest for the R phonon model, as also shown in previous theoretical studies [8,40,41]. In addition, phonon confinement becomes very important in the small range of the well width and it should be considered when investigating the CR absorption FWHM. However, for very large quantum well widths, the FWHMs differ little with the three phonon models and they can be neglected.

References

[1] J.S. Bhat, S.S. Kubakaddi, B.G. Mulimani, J. Appl. Phys. 70 (1991) 2216.
[2] N.L. Kang, J.H. Lee, S.D. Choi, J. Korean Phys. Soc. 37 (2000) 339.
[3] H. Kobori, T. Ohyama, E. Otsuka, J. Phys. Soc. Jpn. 59 (1990) 2141.
[4] M. Singh, Phys. Rev. B 35 (1987) 9301.
[5] B. Tanatar, M. Singh, Phys. Rev. B 43 (1990) 6612.
[6] M.A. Hopkins, R.J. Nicholas, D.J. Barnes, M.A. Brummell, Phys. Rev. B 39 (1989) 13302.
[7] A. Svizhenko, A. Balandin, S. Bandyopadhyay, M.A. Stroscio, Phys. Rev. B 57 (1998) 4687.
[8] S. Rudin, T.L. Reinecke, Phys. Rev. B 41 (1990) 7713.
[9] C.R. Bennett, K. Guven, B. Tanatar, Phys. Rev. B 57 (1998) 3994.
[10] S.G. Yu, K.W. Kim, M.A. Stroscio, G.J. Iafrate, A. Ballato, Phys. Rev. B 50 (1994) 1733.
[11] B.K. Ridley, Phys. Rev. B 39 (1989) 5282.
[12] R. Fuchs, K.L. Kliewer, Phys. Rev. 140 (1965) A2076.
[13] J.J. Licari, R. Evrard, Phys. Rev. B 15 (1977) 2254.
[14] K. Huang, B.-F. Zhu, Phys. Rev. B 38 (1988) 2183.
[15] K. Huang, B. Zhu, Phys. Rev. B 38 (1988) 13377.
[16] Y.J. Cho, S.D. Choi, Phys. Rev. B 49 (1994) 14301.
[17] J.Y. Sug, S.G. Jo, J. Kim, J.H. Lee, S.D. Choi, Phys. Rev. B 64 (2001) 235210.
[18] D. Dunn, A. Suzuki, Phys. Rev. B 29 (1984) 942.
[19] Chuong V. Nguyen, Nguyen N. Hieu, Nikolai A. Poklonski, Victor V. Ilyasov, Le Dinh, Tran C. Phong, Luong V. Tung, Huynh V. Phuc, Phys. Rev. B 96 (2017) 125411.
[20] J.M. Miloszewski, M.S. Wartak, P. Weetman, O. Hess, J. Appl. Phys. 106 (2009) 063102.
[21] S. Melnik, G. Huyet, A.V. Uskov, Opt. Express 14 (2006) 2950.
[22] F. Zhang, L. Li, X.H. Ma, Z.G. Li, Q.X. Sui, X. Gao, Y. Qu, B.X. Bo, G.J. Liu, Acta Phys. Sin. 61 (2012) 054209.
[23] K.D. Pham, L. Dinh, P.T. Vinh, C.A. Duque, H.V. Phuc, C.V. Nguyen, Superlattice Microstruct. 120 (2018) 738.
[24] Khoa Doan Quoc, Hien Nguyen Dinh, Opt. Quant. Electron. 116 (2019) 1.
[25] H. Weman, L. Sirigu, K.F. Karlsson, K. Leifer, A. Rudra, E. Kapon, Appl. Phys. Lett. 81 (2002) 2839.
[26] H. Ham, H.N. Spector, J. Appl. Phys. 90 (2001) 2781.
[27] W.H. Seo, B.H. Han, Solid State Commun. 119 (2001) 367.
[28] C. Matthiesen, A.N. Vamivakas, M. Atature, Phys. Rev. Lett. 108 (2012) 093602.
[29] C.Y. Lin, F. Grillot, N.A. Naderi, Y. Li, L.F. Lester, Appl. Phys. Lett. 96 (2010) 051118.
[30] A. Ulhaq, S. Ates, S. Weiler, S.M. Ulrich, S. Reitzenstein, A. Loffler, S. Hofling, L. Worschech, A. Forchel, P. Michler, Phys. Rev. B 82 (2010) 045307.
[31] N.V.Q. Binh, et al., J. Phys. Chem. Solids 125 (2019) 74.
[32] J.S. Bhat, S.S. Kubakaddi, B.G. Mulimani, J. Appl. Phys. 72 (1992) 4966.
[33] J.S. Bhat, B.G. Mulimani, S.S. Kubakaddi, Phys. Rev. B 49 (1994) 16459.
[34] R. Zheng, M. Matsuura, Phys. Rev. B 61 (2000) 12624.
[35] N.L. Kang, K.S. Bae, C.H. Choi, Y.J. Lee, J.Y. Sug, J.H. Kim, S.D. Choi, J. Phys. Condens. Matter 7 (1995) 8629.
[36] N.D. Hien, Superlattice Microstruct. 131 (2019) 86.
[37] M.P. Chaubey, C.M. Van Vliet, Phys. Rev. B 33 (1986) 5617.
[38] J. Gong, X.X. Liang, S.L. Ban, J. Appl. Phys. 100 (2006) 023707.1.
[39] K.D. Pham, L. Dinh, P.T. Vinh, C.A. Duque, H.V. Phuc, C.V. Nguyen, Superlattice Microstruct. 120 (2018) 738.
[40] Gerald Weber, A.M. de Paula, J.F. Ryan, Semicond. Sci. Technol. 6 (1991) 397.
[41] J.S. Bhat, S.B. Kapatkar, S.S. Kubakaddi, B.G. Mulimani, Phys. Status Solidi 209 (1998) 37.
[42] N.L. Kang, Y.J. Cho, S.D. Choi, Prog. Theor. Phys. 96 (1996) 307.